Journal of Rare Earths 35 (2017) 1180–1185

Contents lists available at ScienceDirect

Journal of Rare Earths

journal homepage: http://www.journals.elsevier.com/journal-of-rare-earths

Preparation and upconversion luminescence modification of $YbPO_4:Er^{3+}$ inverse opal heterostructure☆

Zhuangzhuang Chai, Zhengwen Yang*, Anjun Huang, Chengye Yu, Jianbei Qiu, Zhiguo Song

College of Materials Science and Engineering, Kunming University of Science and Technology, Kunming 650093, China

ARTICLE INFO

Article history:
Received 1 April 2017
Received in revised form
11 June 2017
Accepted 12 June 2017
Available online 24 August 2017

Keywords:
Photonic crystal
Heterostructures
Upconversion luminescence
Modification

ABSTRACT

Photonic crystal heterostructures composed of $YbPO_4:Er^{3+}$ inverse opal and polystyrene opal were prepared via a template-assisted process, which exhibited two photonic band gaps. The microstructure, phase and optical properties of photonic crystal heterostructures were investigated by x-ray diffraction, scanning electron microscopy, fluorescence spectroscopy, absorption spectroscopy, fluorescence lifetime, etc. The upconversion emission suppression caused by single photonic band gap from the following $YbPO_4:Er^{3+}$ inverse opal or the upper opal was observed. The upconversion luminescence was strongly suppressed due to the two photonic band gap overlapping effect caused by the following $YbPO_4:Er^{3+}$ inverse opal or the upper opal. The modified mechanisms of upconversion luminescence were discussed by the upconversion luminescence lifetime of $YbPO_4:Er^{3+}$ photonic crystal heterostructures. The results demonstrated the modified upconversion luminescence is attributed to the photon trapping caused by Bragg reflection of photonic crystal heterostructures.

1. Introduction

Periodical changing of refractive index in photonic crystals (PCs) causes the formation of photonic band gap.[1,2] Photonic band gap can inhibit transmission of light with certain wavelength, which can be used to modify the photoluminescence of active centers embedded in the PCs.[3–9] The photoluminescence modification caused by the PCs has attracted much attention due to the potential applications in high-efficiency diodes and low-threshold lasers, etc., which was demonstrated in the different structural PCs such as opal, inverse opal, diamond, woodpile structure, etc.[3–14] The inverse opal is the ordered spherical pores packed in a solid material, which has excellent photonic band gap properties in contrast to opal prepared by the same material.[15,16] It was well known that most of the rare earth emission light is not monochrome, and the emission color does not match the desired emission. Therefore, one or more methods are required to filter out the undesirable emission. However, conventional tools such as filters and other devices are too cumbersome. The inverse opal photonic crystal structure is capable of modulating the corresponding emission due to its photonic band gap characteristics. Compared to conventional filter materials, the advantage of inverse opal is that it is the luminescence and filter medium in itself. By doping the inverse opals with rare earth ions, the photonic band gap of inverse opals can modify the photoluminescence of rare earth ions.[17–19] However, many previous researches focused on the influence of single photonic band gap of inverse opal on the photoluminescence.[18,19] In addition, this modification is not particularly significant. The reason is that photonic band gap has its special character, which can only modify the luminescence of rare earth ions embedded inside the inverse opal. The photoluminescence of rare earth ions at the inverse opal surface could not be modified by its photonic band gap. Therefore, further enhancing the photoluminescence modification of rare earth ions embedded in the inverse opal is important for their application potentials.

The PCs heterostructure is composed of two or more layers PCs, which has two or more photonic band gaps.[20] The PCs heterostructure can be further used to improve the photoluminescence modification of rare earth ions embedded in the PCs. The photoluminescence of rare earth ions at the surface of following layer PCs

---

☆ **Foundation item:** Project supported by the National Natural Science Foundation of China (11674137), the Applied Basic Research Program of Yunnan Province (2014FB127), Reserve Talents Project of Yunnan Province (2012HB068) and Talent Youth Science Foundation of College of Materials Science and Technology, Kunming University of Science and Technology (20140205).

* Corresponding author.
E-mail address: yangzw@kmust.edu.cn (Z.W. Yang).

http://dx.doi.org/10.1016/j.jre.2017.06.009

could be modified by the photonic band gap of upper layer PC. In the present work, the heterostructure composed of the $YbPO_4:Er^{3+}$ inverse opal and an opal was prepared by the self-assembled method. The influence of photonic band gap of PCs heterostructure on the upconversion (UC) luminescence of Er^{3+} was investigated. The results demonstrated that the green and red UC luminescence of Er^{3+} was further suppressed by the PCs heterostructure, which can act as the purifier of UC emission color.

2. Experimental

The $YbPO_4:Er^{3+}$ PCs heterostructure that consisted of $YbPO_4:Er^{3+}$ inverse opal and polystyrene (PS) opal were synthesized by the self-assembled method. First, the opal PCs composed of the monodispersed 300, 350 or 450 nm PS microspheres were prepared by the vertical deposition process, respectively.[21–23] Second, the $YbPO_4:Er^{3+}$ sol was prepared by using Yb_2O_3, Er_2O_3, P_2O_5 and nitric acid as raw material. The Yb_2O_3 and Er_2O_3 dissolved into the hot nitric acid were evaporated to dryness to obtain ytterbium and erbium nitrification. The ytterbium, erbium nitrification and P_2O_5 were dissolved in anhydrous ethanol, respectively. The above solution was mixed uniformly by a uniform stirring to obtain $YbPO_4:Er^{3+}$ sol. Third, the $YbPO_4:Er^{3+}$ sol was infiltrated into the opal PCs, which was sintered at 900 °C in an air atmosphere for 5 h, and $YbPO_4:Er^{3+}$ inverse opals were prepared. Finally, the prepared $YbPO_4:Er^{3+}$ inverse opals were inserted into the volumetric flasks containing 230 or 270 nm PS microspheres, which were held at the 55 °C for several days. The opal was formed on the surface of $YbPO_4:Er^{3+}$ inverse opal, and the $YbPO_4:Er^{3+}$ PCs heterostructure consisted of $YbPO_4:Er^{3+}$ inverse opal and PS opal was obtained.

The UC photoluminescence measurement of $YbPO_4:Er^{3+}$ PC heterostructures was carried out on a Hitachi F-7000 spectrophotometer upon the 980 nm excitation. The transmission spectra of $YbPO_4:Er^{3+}$ PCs heterostructures were measured by Hitachi U-4000 spectrophotometer. The morphologies and structures of $YbPO_4:Er^{3+}$ inverse opal and $YbPO_4:Er^{3+}$ PC heterostructures were inspected by using a scanning electron microscope (SEM). The phase purity and crystallinity of $YbPO_4:Er^{3+}$ inverse opals were examined by powder X-ray diffraction (XRD) performed on a D/max-2200 diffractometer. The spectra of UC luminescence decay were recorded on a FLSP-980 spectrophotometer.

3. Results and discussion

The $YbPO_4:Er^{3+}$ inverse opals prepared by the PS opals composed of the 300, 350 and 450 nm PS microspheres were denoted as the IO-I, IO-II and IO-III, respectively. Fig. 1 exhibits the X-ray diffraction patterns of the IO-I, IO-II and IO-III after the removing of PS microspheres. The XRD diffraction peaks located at 19.75°, 26.12° and 37.27° were indexed as (101), (200) and (112) lattice plane, respectively, which indicated that the tetragonal phase $YbPO_4:Er^{3+}$ inverse opal was prepared. By using the Debye–Scherrer equation, the crystalline grain size of the IO-I, IO-II and IO-III was estimated by the half maximum width of 26.12° diffraction peak, which is about 35.71, 38.27 and 41.47 nm, respectively.

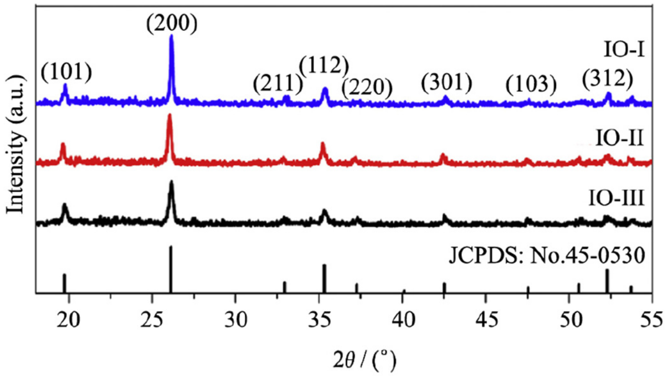

Fig. 1. XRD patterns of IO-I, IO-II and IO-III.

Fig. 2(a)–(c) exhibits the surface SEM images of the IO-I, IO-II and IO-III, respectively. The order packing of air spheres with hexagonal configuration was observed in each $YbPO_4:Er^{3+}$ inverse opal. For the IO-I, IO-II and IO-III, the distance between two near air sphere estimated by SEM image is about 227, 278, and 336 nm, respectively, which is smaller than the diameter of original PS microspheres. About 24.4%, 22.6% and 25.4% shrinkage occurs for the IO-I, IO-II and IO-III due to the removal and decomposition of PS microspheres. The IO-I, IO-II and IO-III were inserted into the flasks containing 230 or 270 nm PS microspheres, respectively. By further self-assembling, the opal composed of the 230 or 270 nm PS microspheres was formed on the surface of IO-I, IO-II and IO-III, respectively, and the PCs heterostructures consisted of $YbPO_4:Er^{3+}$ inverse opal and PS opal were obtained. The IO-I and IO-II after the formation of 230 nm PS opal were denoted as the IO-I-230 and IO-II-230, respectively. The IO-I and IO-III after the formation of 270 nm PS opal were denoted as the IO-I-270 and IO-III-270, respectively. The SEM images of the surface of IO-I-230, IO-I-270, IO-II-230 and IO-III-270 are presented in Fig. 2(d)–(g), respectively. The order structure of PS opal was demonstrated by the SEM images in each case. Fig. 2(h) exhibits the cross sectional SEM images of IO-I-230. It is noted that obvious interface between the inverse opal and opal is observed, and the PCs heterostructures that consisted of $YbPO_4:Er^{3+}$ inverse opal and PS opal were prepared successfully.

Fig. 3(a) shows the absorption spectra of IO-I, IO-II and IO-III at normal incident of light. The maximum absorption of the IO-I, IO-II and IO-III represent the photonic band gap position, which was attributed to the Bragg reflection of ordered lattice planes. The photonic band gap for the IO-I, IO-II and IO-III was located at 430, 535 and 645 nm, respectively. Fig. 3(b) shows the absorption spectra of IO-I-230, IO-I-270, IO-II-230 and IO-III-270. Two photonic band gaps from the following inverse opal and upper PS opal were observed in the IO-I-230 and IO-I-270, respectively. The photonic band gap from the upper PS opal was located at the 538 and 655 nm in the IO-I-230 and IO-I-270, respectively. Theoretically, the Bragg's diffraction law $\lambda = 1.633D\,(n^2_{\text{eff}} - \sin^2\theta)^{1/2}$ could be used to determine the photonic band gap position of the inverse opal or opal PCs. In the Bragg's law, the θ and D is the incidence angle of light with respect to the PCs normal line and the periodical size of PCs (for the opal, D is the diameter of PS microspheres; for the inverse opal, D is the distance between two near air sphere). The refractive index of PCs (n^2_{eff}) can be determined by the following equation: $n^2_{\text{eff}} = n^2 f + n^2_{\text{air}}(1 - f)$. The n_{air} is the refractive index of air ($n_{\text{air}} = 1$). The n is the refractive index of PS microspheres in the opal ($n = 1.59$) or $YbPO_4$ in the inverse opal ($n = 1.68$). The f is the volume fraction of PS microspheres for the opal ($f = 74\%$) or $YbPO_4$ for the inverse opal ($f = 26\%$). The photonic band gap of IO-I, IO-II and IO-III calculated by the Bragg's law was located at 441, 533 and 652 nm, respectively. The photonic band gap of opal composed of the 230 and 270 nm is at 550, 642 nm, respectively. Fig. 3(c) exhibits a comparison of the measured photonic band gap of opal or inverse opal with these calculated by the Bragg's law, which shows the calculated and measured results are similar. For the IO-II-230 and IO-III-270 samples, only one photonic band gap was observed because the photonic band gap from the